NASA TECHNICAL MEMORANDUM

NASA TM X-62,274

NASA TM X-62,274

STUDY OF THE FAR WAKE VORTEX FIELD GENERATED BY A RECTANGULAR AIRFOIL IN A WATER TANK

Dietrich K. Lezius

Ames Research Center
Moffett Field, Calif. 94035

May 1973

STUDY OF THE FAR WAKE VORTEX FIELD GENERATED BY A RECTANGULAR AIRFOIL IN A WATER TANK

Dietrich K. Lezius*
Ames Research Center, NASA
Moffett Field, CA 94035

Abstract

Underwater towing experiments were carried out with a rectangular airfoil of aspect ratio 5.3 at 4° and 8° angles of attack and at chord-based Reynolds numbers between 2×10^5 and 7.5×10^5. Quantitative measurements by means of the hydrogen bubble technique indicated lower peak swirl velocities in the range of 100 to 1000 chord lengths downstream than have been measured in wind tunnel or flight tests. The maximum circumferential velocity decayed as $t^{-7/8}$, whereas the turbulent eddy viscosity, ν_T, increased as $t^{3/4}$. This behavior and other known rates of vortex decay are explained in terms of an analytical solution for the vortex problem with time varying eddy viscosity. It is shown that this case corresponds to nonequilibrium turbulent vortex flow which has other self similar solutions, such that the rate of vortex decay is greater than $t^{-1/2}$ when the eddy viscosity increases with time. Conversely, the decay proceeds at a rate less than $t^{-1/2}$ when ν_T decreases with time.

Notation

a	= core radius
b	= wing span
c	= wing chord
ΔH	= head loss in boundary layer
m	= exponent for time varying eddy viscosity
p	= pressure
p_∞	= fluid pressure as $r \to \infty$
$p(0)$	= pressure on the vortex axis
P	= rate of turbulent energy production
r	= radius measured from vortex axis
s	= tangential shear deformation, $s = \partial v/\partial r - v/r$
t	= time
Δt	= time difference in velocity measurement
T	= time parameter, $T = \Gamma_\infty t/c^2$
u	= radial velocity component
U_∞	= towing speed
v	= tangential velocity component
v_a	= tangential velocity at $r = a$
$\overline{u'v'}$	= Reynolds stress
w	= axial velocity component
w_0	= axial velocity on vortex axis
z	= downstream distance behind airfoil
α	= angle of attack
β	= constant of proportionality, Eq. (10)
Γ	= circulation
Γ_a	= circulation at core radius
Γ_∞	= circulation of wing
$\theta, \Delta\theta$	= angle in velocity measurement
ν	= kinematic viscosity
ν_e	= effective viscosity
ν_T	= eddy viscosity
$(\nu_T/\nu)_a$	= eddy viscosity at core radius
$(\nu_T/\nu)_0$	= eddy viscosity level after roll up
ρ	= density
τ	= turbulent shear stress

*Research Associate, National Research Council, 1970/72, Ames Research Center, NASA, Moffett Field, CA.

Introduction

With the advance of the heavy transport jet planes such as the 747, and more recently the DC-10 and L-1011, a rather intense theoretical and experimental effort has been directed toward the problem of "wake turbulence." This so-called turbulence, also known as turbulent wake, consists of the remains of a system of counter rotating wing tip vortices which are shed from the aircraft as part of the generation of lift. When a following plane enters the vortex wake it can, depending upon its size, be rolled out of control or, in the more severe cases, even suffer serious structural damage.

The intensity and longevity of vortex wakes increase with the weight of the aircraft generating the wake, but in general, the severity of the upset is proportional to the swirl momentum left in an effective cross sectional area of the wake at the time of encounter. Since the wake vortices dissipate in time as a result of turbulent and atmospheric effects, an encounter with an "old" wake is expected to induce less severe roll on the following craft than one with a newly formed wake. Present aviation rules call for several miles separation between planes on approach, so that possible encounters would occur in the far field of the wake where the separation between planes is on the order of 10^3 or more mean chord lengths. There are, however, strong incentives toward closer aircraft spacing and hence toward increased hazards from encounters with vortex wakes.

In several recent wind tunnel studies, most notably those of Chigier and Corsiglia,[1,2] Logan,[3] and Mason and Marchman,[4] tangential and axial velocity components of the vortex field were measured after roll up. Subsequent velocity distributions and initial rates of decay of the flow field were obtained for downstream distances up to $z/c = 30$, and can thus be regarded as data from the near and intermediate fields of the wakes.

Although flight measurements of maximum tangential vortex velocities acquired as far back as 7000 chord lengths have been reported by McCormick et al.,[5] no such data are available for comparison from model tests where the dynamics of vortex decay in the far field can be studied under well controlled conditions. Since in-flight encounters with vortex wakes are most likely to occur in the far field, a better understanding of the mechanics and the structure of wake vortex flow in the late stage is required.

The purpose of the present paper is to report on a series of underwater towing experiments which allowed measurements in the far wake region of a rectangular NACA-0015 airfoil of 0.915 meter span with rounded wing tips and aspect ratio 5.33. Chord-based airfoil Reynolds numbers ranged from 2.2×10^5 to 7.5×10^5, and angles of attack were set at 4° and 8°. Use of the hydrogen bubble technique** permitted

**This technique uses hydrogen bubbles generated by electrolysis on a metal wire to mark the flow.

visual observations of the development of the turbulence structure in the core and the potential regions during vortex decay. Simultaneously, the flow was photographed on 16 mm movie film from an axial and a crosswise viewing direction. Quantitative measurements were made from these films of the tangential velocity profiles and maximum axial velocity. Thus, rates of vortex growth measured at the core and decay of the maximum tangential velocity were established as a function of chord-based downstream distance.

In the last section of this paper, a closed-form solution is obtained for the vortex decay with time varying eddy viscosity, which affords determination from the data of eddy viscosity levels in the vortex flow at given points in time. This information is then used to compute radial distributions of turbulent shear stress and rates of production of turbulence energy.

Experimental Procedure

The towing tests were conducted in the Lockheed Underwater Missile Facility (4.6 m x 4.6 m x 55 m) with the airfoil mounted to a towing carriage by a streamlined strut (see Fig. 1). The hydrogen bubble generating wire consisted of three twisted platinum wires, 4.6 μ dia, and was mounted within the tank at an angle to the vertical and below the right wing tip. A 5 kw light source mounted above the tank was capable of illuminating the plane of the platinum wire with an intense light sheet, 1.2 m x 0.3 m in cross section. Two cameras were mounted at the elevation of the airfoil, one of which was lined up within the plane of the platinum wire; the view of the other camera was pointed in the axial direction by use of a mirror.

Side view and axial view film recordings of the right vortex were made in two modes, one in which hydrogen bubbles were generated at the rate of 3/sec from the moment of passage of the airfoil until the vortex flow field was well marked. This mode of operation, illustrated in Fig. 2, yielded excellent photographs for further visual study. In the second mode, lines of hydrogen bubbles were only pulsed while the vortex core crossed the wire, so that they were not obscured by previously marked fluid. These lines, also visible in Fig 2, served for measurement of the tangential velocity profiles. For the purpose of velocity measurements, the age of the vortex was determined by the time elapsed between passage of the airfoil and the instant at which the vortex core crossed the wire. The center of the core, or vortex filament, was usually well marked by hydrogen bubbles left in the water from the previous run.

Discussion of Results

Tangential Velocity and Circulation

The method of obtaining velocity profiles by means of the hydrogen bubble technique in a linear flow is described in detail by Schraub et al.[6] In the present work, radial velocity distributions were deduced from film by measuring from the center of the vortex the polar coordinates of the hydrogen bubble time line next to the wire, whereby the downward motion of the vortex system, given by $\Gamma_\infty/2\pi b$, was neglected. Since the time delay, Δt, between time lines is known from the film frame speed, the tangential velocity variation is given by

$$v(r) = \frac{r\Delta\theta}{\Delta t} \qquad (1)$$

This procedure is indicated schematically in Fig 3. After computation of v(r) for each side of the vortex, the results were averaged in order to represent the vortex by one velocity profile.

Typical velocity profiles, normalized on the towing speed, U_∞, are shown in Fig 4 for 4° and 8° angles of attack. The radius is normalized on the wing span, b. The velocity profiles decay with downstream distance in a manner quite similar to a laminar vortex; this point will be discussed further in a later section. The reduction in maximum tangential velocity proceeds with a simultaneous enlargement of the core. Outside the core, the tangential velocity approaches the envelope of the potential vortex, but it should be noted that due to viscous or turbulent shear forces, the flow field decays everywhere simultaneously.

Fig 5 shows the decay of the maximum tangential velocity for the range of downstream distance investigated in this study. For comparison, we also list the flight test data of McCormick et al.,[5] which was normalized appropriately. The effect of angle of attack upon v_a/U_∞, shown in the flight test data* and also noted in Refs. 2, 5, and 7 for short distances behind the wing, has disappeared from our data for the downstream distances investigated. As will be shown in the discussion of turbulent contributions to vortex decay, higher levels of turbulence, or eddy viscosity, were produced at higher angles of attack. The result was an increased rate of decay of v_a, which tended to diminish the differences in maximum tangential velocities caused by the dependence upon α. The data indicate, furthermore, that for z/c above 300, the rate of decay of the maximum swirl velocity approached a slope of -7/8. This rate is considerably higher than the $t^{-1/4}$ dependence exhibited by the flight test data of McCormick et al.,[5] for large distances behind the airfoil. Using the notion that turbulent diffusion is proportional to the root mean square of the turbulent fluctuations, Brown[8] concluded that the turbulent vortex decay should follow as $t^{-1/3}$, hence $(z/c)^{-1/3}$, indicating a slower rate of vortex decay than that usually observed. The computations by Baldwin et al.[9] on turbulent vortices, however, showed that turbulent diffusion contributes significantly only in regions of low shear. Brown's analysis, applied to the region of the core radius, does not adequately explain the vortex spreading rate, since the turbulent shear stresses are maximum just outside this region. Examination of the present velocity data with respect to eddy viscosity levels within the trailing vortex showed that the high rates of decay and transport of core angular momentum outward were, in fact, due to the increase of the eddy viscosity with time. This discussion is deferred until a later section.

The growth of the vortex core region with downstream distance is illustrated in Fig. 6. The indicated growth rate proportional to $(z/c)^{2/3}$ for the data at 4° agrees only coincidentally with the vortex spreading rate proposed by Brown. As mentioned above, the rate of radial transfer of angular momentum is related to changes of the eddy viscosity with time. The higher growth rate observed at 8°

*It is estimated that within the flight data of McCormick et al.,[5] the angle of attack varied by a factor of two.

angle of attack is found to be the inverse of the rate of vortex decay deduced from Fig. 5, but this condition need only be satisfied if we require that the product $v(a,t)a(t)$ remain invariant with time. The faster spreading of the core angular momentum can be associated with higher turbulence levels in the vortex after roll up and with increased rates of turbulence production by the mean shearing deformation outside the core.

Typical circulation profiles as a function of downstream distance are shown in Fig. 7. The trend toward self similarity, also evident in the velocity profiles, is well demonstrated by the data. Overshoot of the circulation was observed in some cases and may have been related to radial variations in the rate of turbulent momentum transport, as discussed by Govindraju and Saffman.[10]

Hoffman and Joubert[11] proposed a universal correlation of $\Gamma(r)/\Gamma_a$ vs log (r/a). Fig. 8 shows the present circulation data in these coordinates. It is noted here that this curve expresses merely the self similar property of the circulation profiles, but it cannot be regarded as a correlation of the flow on characteristic turbulence quantities. In the area of the core, the centrifugal force field exerts a pronounced damping effect upon the turbulent mixing process, thereby decreasing the length scale of turbulent momentum exchange. Donaldson[12] pointed out that the use of eddy transport models does not lend sufficient generality to the development of turbulence in aircraft trailing vortices. This shortcoming accounts for the considerably narrowed extent of the logarithmic region ($0.6 < a < 1.3$) when compared with the logarithmic law of the turbulent boundary layer.

The value of the circulation at the location of maximum tangential velocity has been the point of much previous discussion. When the vortex decays under the effect of constant molecular viscosity, Lamb's[13] solution yields the value $\Gamma_a/\Gamma_\infty = 0.715$. In the work of other investigators (see Ref. 10), the value of Γ_a/Γ_∞ ranged from 0.37 to 0.6, and the model of Govindraju and Saffman[10] allows for $\Gamma_a/\Gamma_\infty = 1.2$. In the recent vortex measurements with a laser velocimeter by Orloff and Grant[7] at $z/c = 2$ behind a rectangular wing, the core circulations varied between 0.2 and 0.8 x Γ_∞, depending upon the angle of attack. The wind tunnel measurements of Corsiglia et al.[14] resulted in $\Gamma_a/\Gamma_\infty \approx 0.4 - 0.5$. Donaldson's[12] calculations indicate a slight decrease with time of the initial circulation at the core, whereas McCormick et al.[5] proposed that when a decaying vortex maintains geometric similarity, Γ_a/Γ_∞ = constant. This conclusion seems to be confirmed by the data presented herein. Fig. 9 shows that the circulation at the core radius remained essentially constant with downstream distance at an average value of $\Gamma_a/\Gamma_\infty = 0.67$. The values plotted in Fig. 9 were determined by two different methods: with the first method, Γ_a/Γ_∞ was obtained directly from plots of Γ/Γ_∞ vs r/b; the second method involved measuring the slope of Γ/Γ_∞ plotted vs log (r/b), since

$$\left[\frac{d\Gamma(r)/\Gamma_\infty}{d\ln(r/b)}\right]_{r=a} = \frac{\Gamma_a}{\Gamma_\infty} \qquad (2)$$

It should be noted that much of the Γ_a data gathers around the theoretical value of 0.715 for constant eddy viscosity. A comparison of these data with calculations of ν_T/ν from the circulation profiles (see Eq. 17) indicated that the low values for Γ_a were associated with runs in which ν_T/ν increased in the radial direction at the location of the core radius. For the remaining cases it was found that ν_T/ν did not depend on r.

Axial Velocity

The importance of the axial core velocity has been previously discussed by Batchelor,[15] Brown,[8] and Saffman.[16] As a result of these studies, it has become evident that the axial velocity in the core can be directed either toward the wing or away from it, depending upon a balance between the viscous airfoil drag, which causes a wake to form, and the swirl induced radial pressure gradient, which tends to propel the core fluid as a jet down the cortex core. Batchelor's formulation for the radial variation of the axial velocity, expressed in coordinates of a stationary observer, is given by

$$w(r) = \frac{1}{2\pi}\int_r^\infty \frac{\partial\Gamma^2(r)}{\partial r}\,dr - 2\Delta H \qquad (3)$$

where ΔH is the head loss due to the viscous boundary layer on the wing. If the viscous drag term is larger than the integral term, as is the case at moderate angles of attack, one observes a velocity defect in the core. However, the data of Chigier and Corsiglia[2] show a reversal from a wake flow in the core to an axial velocity excess, measured at a downstream distance of $z/c = 9$, when the angle of attack increases from 8° to 12°. Hence, at large angles of attack, the swirl induced pressure drop along the vortex axis immediately behind the wing is strong enough to accelerate fluid from the wing tip area in the downstream direction, despite the momentum loss incurred by passing through the viscous boundary layer.

In the present experiments, quantitative axial velocity profiles were difficult to obtain, but the visual studies revealed velocity defects in the core at 4° and 8° angles of attack. The most notable feature of the axial flow was the presence of a sharp radial peak in the axial velocity profile near the vortex axis. This observation qualitatively agrees with the theoretical results of Brown[8] regarding the roll up of the momentum deficient boundary layer fluid into the vortex. Accordingly, the axial velocity profile, whether representing a wake or a jet, assumes a $1/r$ dependence through the core.

Measurements of the axial velocity on the axis were made by following fine lines of entrained hydrogen bubbles which marked the vortex filaments in many cases. The magnitude of the maximum defect velocity depended strongly upon the angle of attack, as shown in Fig. 10. These measurements, furthermore, revealed that the velocity on the vortex axis accelerated to a maximum before decaying with time. Acceleration of the axial flow was accompanied by strong radial flow toward the axis in the core region. The mechanism for acceleration of the axial flow may be related to a streamwise pressure rise resulting from the decay of the integral for the radial pressure gradient:

$$p(0) - p_\infty = -\rho\int_0^\infty \frac{v^2(r)}{r}\,dr \qquad (4)$$

Since the stationary observer sees a velocity profile that decays with time, we have for the pressure gradient in fixed coordinates:

$$\frac{\partial p(0)}{\partial z} = -\rho \frac{\partial}{\partial z}\int_0^\infty \frac{v^2(r)}{r}\,dr = -\frac{1}{\rho U_\infty}\int_0^\infty \frac{2v}{r}\left(\frac{\partial v}{\partial t}\right)dr > 0 \quad (5)$$

where we made the transformation $z = U_\infty t$. The fluid surrounding the axis would thus tend to accelerate toward the low pressure region behind the wing. With increasing time, the axial pressure gradient is diminished, while viscous and turbulent friction cause the axial flow to slow down.

The initial acceleration of the axial flow toward the wing at moderate angles of attack assumes significance in regard to the stability of the vortex core, that is, its resistance to turbulent eddies diffusing from the outer core region inward. Letting the swirl velocity be invariant in the azimuthal direction and setting again $z = U_\infty t$, the equation of continuity is given by

$$\frac{1}{r}\frac{\partial(ru)}{\partial r} + \frac{1}{U_\infty}\frac{\partial w}{\partial t} = 0 \quad (6)$$

If we assume a mean value for the axial acceleration in the core, $\overline{\frac{\partial w}{\partial t}}$, the radial inflow, u(r), is approximated by

$$u(r) \approx -\frac{r}{2U_\infty}\overline{\frac{\partial w}{\partial t}} \quad (7)$$

The momentum equation for the tangential flow is

$$\frac{\partial v}{\partial t} + u\frac{\partial v}{\partial r} + \frac{uv}{r} + \frac{w}{U_\infty}\frac{\partial v}{\partial t} = 0 \quad (8)$$

Inside the core, $\frac{\partial v}{\partial r} \approx \frac{v}{r}$, so that by combining Eqs. (7) and (8), we obtain for the rate of change of the tangential core velocity

$$\frac{1}{v}\frac{\partial v}{\partial t} \approx \frac{1}{U_\infty(1 + w/U_\infty)}\left(\overline{\frac{\partial w}{\partial t}}\right) \quad (9)$$

Hence, spin up of the core angular velocity is induced by acceleration of the axial core flow. The vortex filament is thereby strengthened and further stabilized. This phenomenon may be partly responsible for the reported persistence over long periods of time of well defined cores of aircraft trailing vortices.

Effect of Turbulent Viscosity on Vortex Decay

Theoretical Considerations

It is generally agreed that the effective, or turbulent eddy viscosity, ν_T, present in the vortex is considerably higher than the molecular viscosity, and thus contributes to the rate of vortex decay. According to data from various investigators collected by Owen,[17] estimates for ν_T/ν fall between 30 and 2000, depending upon the vortex Reynolds number, Γ_∞/ν. Kuhn and Nielsen,[18] for instance, proposed a theory to calculate the vortex decay by using the z-component of the eddy viscosity evaluated at the vortex axis. Their predictions fit the wind tunnel data of Chigier and Corsiglia[2] for values of the eddy viscosity ratio between 200 and 450. Squire[19] suggested that Lamb's laminar solution can still be applied to the turbulent vortex decay when the eddy viscosity is constant with time and the radial coordinate, and is given by

$$\nu_T = \beta\Gamma_\infty \quad (10)$$

Owen proposed a more sophisticated model, but in order to achieve agreement with experiment, also finally assumed that ν_T is proportional to Γ_∞. Both models result in a rate of decay of v_a proportional to $t^{-1/2}$.

However, different rates of vortex decay have been previously observed, which, together with the data of this study, suggest that the eddy viscosity may vary with time. Particularly in towing experiments, where the airfoil is moved through an undisturbed fluid, one may expect an initial increase of the eddy viscosity and a corresponding contribution to the rate of vortex decay. This reasoning seems logical in view of the fact that the fluid is initially free of turbulence, and that the rolled up boundary layer from the airfoil does not account for the turbulence levels found in the vortex field at some later time. In wind tunnel tests, and particularly in flight test situations where propulsion thrust contributes to the initial turbulence, one would expect a decay of the initial turbulence with time, and hence a decay rate for v_a slower than $t^{-1/2}$. Lilley's[20] examination of the experimental flight data of Rose and Dee[21] with respect to time varying eddy viscosity led to a decay of the maximum tangential velocity according to $t^{-1/3}$. In the work of Baldwin et al.[9] on turbulent flow calculations, it was pointed out that the vortex initially is a non-equilibrium flow, i.e., turbulence production ≠ dissipation. Thus their calculated eddy viscosity decreased sharply from the initial value ($\approx 0.5\times10^3$) and then reached a constant of $\nu_T/\nu \approx 150$. It is interesting to observe that during this time, the circumferential velocity attained only a very small decay rate. As ν_T/ν approached a constant or presumably an equilibrium value, the maximum tangential velocity reached the familiar dependence upon $t^{-1/2}$.

The following describes an analytical solution for the decay of an originally potential vortex with turbulence when the eddy viscosity is allowed to vary with time, but remains constant in the radial direction. Since the actual development of turbulence in the vortex flow is not considered, the solution shows the dependence of the rate of vortex decay upon particular assumed variations in $\nu_T(t)$ which are actually observed.

We define the effective viscosity of the flow

$$\nu_e \equiv \nu + \nu\left(\frac{\nu_T}{\nu}\right)_0 T^m = \nu\left[1 + \left(\frac{\nu_T}{\nu}\right)_0 T^m\right] \quad (11)$$

where $(\nu_T/\nu)_0$ is the initial eddy viscosity level in the flow after roll up. The symbol, T, is dimensionless time using appropriate parameters of the flow, e.g., $T = t\Gamma_\infty/c^2$. In order to solve the resulting differential equation, we make the further assumption that $(\nu_T/\nu)_0 T^m \gg 1$. This assumption is justified in wind tunnel and flight tests, except perhaps in low Reynolds number towing experiments. Under these circumstances, the two-dimensional vortex motion is governed by

$$\frac{\partial v}{\partial t} = \nu\left(\frac{\nu_T}{\nu}\right)_0\left(\frac{\Gamma_\infty t}{c^2}\right)^m\left[\frac{\partial^2 v}{\partial r^2} + \frac{1}{r}\frac{\partial v}{\partial r} - \frac{v}{r^2}\right] \quad (12)$$

The solution to this equation is

$$v(r,t) = \frac{\Gamma_\infty}{2\pi r}\left[1 - \exp\left(-\frac{(m+1)r^2}{4\nu\left(\frac{\nu_T}{\nu}\right)_0\left(\frac{\Gamma_\infty t}{c^2}\right)^m t}\right)\right] \quad (13)$$

We note that the overall features of the flow remain the same as with constant ν_T; but the rate of change with time now depends upon the development of the eddy viscosity. We want to establish the rate of change of the maximum circumferential velocity and the growth of the vortex core as m assumes various values. Solving for the radius at the point of maximum tangential velocity, a(t), and substituting r = a(t) in equation (13), we have

$$v(a,t) \sim U_\infty\left(\frac{\Gamma_\infty t}{c^2}\right)^{-(m+1)/2} \quad (14)$$

and

$$a(t) \sim b\left(\frac{\Gamma_\infty t}{c^2}\right)^{(m+1)/2} \quad (15)$$

In contrast to vortex decay with constant ν_T, the growth of the vortex is proportional to $t^{(m+1)/2}$, i.e., time dependent changes in ν_T contribute to the rate of vortex decay through the additional exponential factor m/2. Table 1 demonstrates the significance of these results.

Table 1. Time dependence of maximum circumferential velocity and core radius upon assumed time variation of ν_T/ν.

m	-1	-2/3	-1/3	0	1/3	2/3	1
v(a,t)	~ 1	$\sim t^{-1/6}$	$\sim t^{-1/3}$	$\sim t^{-1/2}$	$\sim t^{-2/3}$	$\sim t^{-5/6}$	$\sim t^{-1}$
a(t)	~ 1	$\sim t^{1/6}$	$\sim t^{1/3}$	$\sim t^{1/2}$	$\sim t^{2/3}$	$\sim t^{5/6}$	$\sim t$

Surveying the literature, including the results of this study, one finds that the range of time decay factors listed in Table 1 include those either previously measured or predicted using various theories of turbulent shear flow. The case m = -1 is of interest since turbulent vortex decay initially behaves remarkably in this way, namely with no appreciable decay of the circumferential velocity or growth of core radius. The initial value of m, of course, does not remain constant but tends toward zero at the same rate at which equilibrium conditions are established in the vortex flow. On the other hand, the calculations of Baldwin et al. showed that the $t^{-1/2}$ dependence occurred from the outset when the initial conditions were chosen corresponding to an equilibrium flow. The authors called these solutions self similar, but we recognize that all solutions with constant m possess the self similar property. Hence, m = 0 represents the law for turbulent vortex decay when equilibrium conditions have been established in the flow. The available data on wake vortices suggest strongly that the time required to reach this condition is proportional to the degree to which the initial flow conditions deviated from those of equilibrium.

In view of the findings above, our test results in a towing tank suggest primarily that the turbulence intensities were rising during the development of the vortex, but had not reached the equilibrium level which is characteristic of the dependence upon $t^{-1/2}$. This conclusion derives from the result that the rate of vortex decay remained proportional to $t^{-7/8}$. For the rate of change of the eddy viscosity with time, we obtain from Eq. (14) and the data in Fig. 5 that m = 3/4, and thus $(\nu_T/\nu)_a \sim t^{3/4}$. Using the appropriate equations given in the papers of Baldwin et al.[9] and Donaldson[12] we estimated the equilibrium eddy viscosity level to be $(\nu_T/\nu)_{equ.} \approx 150$.

Experimental Results

The variation of ν_T/ν with radius and time was computed from a graphical fit to the circulation profiles. Substituting

$$\nu_T/\nu = \left(\frac{\nu_T}{\nu}\right)_0\left(\frac{\Gamma_\infty t}{c^2}\right)^m \quad (16)$$

in Eq. (13) and solving for ν_T/ν, we have

$$\frac{\nu_T(t)}{\nu} = -\frac{(m+1)r^2}{4\nu t \ln\frac{\Gamma_\infty - \Gamma(r,t)}{\Gamma_\infty}} \quad (17)$$

Using m = 3/4 as established from the data of Fig. 5, profiles computed from Eq. (17) were accepted as representing levels of the eddy viscosity approximately when ν_T/ν was invariant with r, or nearly so, at the location of the core radius. Surprisingly, this condition was satisfied in the majority of the examined vortex profiles. Some typical results are shown in Fig. 11, indicating an expected dependence upon Γ_∞ through α and U_∞. A summary of the eddy viscosity data obtained at the location of the core radius is plotted in Fig. 12, together with the wind tunnel data of Refs. 18, 22-25. It is seen that the eddy viscosity levels in the towing experiments were below those obtained in wind tunnel tests.

Fig. 13 shows the time dependence of eddy viscosity, $(\nu_T/\nu)_a$, determined at the radius of maximum tangential velocity for the data taken at $\alpha = 8°$. The indicated increase of $(\nu_T/\nu)_a$, proportional to $t^{3/4}$, is in agreement with the value of m established from the slope in Fig. 5.

Interaction of the turbulent shear stress, $\tau/\rho = -\overline{u'v'}$, with the mean flow provides the significant mechanism for dissipation of the mean flow energy via production of turbulence. Nondimensional turbulent shear stress profiles were computed from

$$\frac{\tau/\rho}{\Gamma^2/b^2} = \frac{\nu_T}{\Gamma^2/b^2}\left(\frac{\partial v}{\partial r} - \frac{v}{r}\right) \quad (18)$$

Fig. 14 shows shear stress profiles for $\alpha = 8°$ at various downstream distances. They agree with the computed results of Donaldson and Baldwin et al. in shape and the relative location of the peak value with respect to the core radius. Rates of production of turbulent kinetic energy, normalized upon Γ_∞^3/b^4, were computed from

$$P = -\frac{\tau/\rho\left(\frac{\partial v}{\partial r} - \frac{v}{r}\right)}{\Gamma^3/b^4} \quad (19)$$

Fig. 15 shows representative profiles of turbulence production for the conditions of Fig. 14 in relation

to downstream distance. At the core radius, P attains approximately one-half its peak value. It is also evident that as the core radius grows, decreasing portions of the mean flow energy are dissipated in the core due to the increasing region of solid body rotation.

Concluding Remarks

Using a towing tank facility, tangential velocity profiles were measured far downstream of a rectangular air foil. The resulting rates of decay of the maximum tangential velocity followed a $t^{-7/8}$ dependence, and rates of growth of the vortex core were also greater than expected. Analysis of the data showed that this particular behavior was related to the increase in the turbulent eddy viscosity with time; specifically, ν_T/ν appeared to increase according to $t^{3/4}$. Values of circulation measured at the point of maximum circumferential velocity, although scattered, remained constant in the mean with downstream distance at about 0.67 Γ_∞. High axial velocities with initial acceleration in the towing direction were observed and were attributed to a strongly stabilizing influence upon the vortex filament.

An analytical solution to the problem of vortex decay with time varying eddy viscosity revealed that only under equilibrium flow conditions does the self similar solution for the tangential velocity depend upon $t^{-1/2}$. Wind tunnel and flight test data, as well as flow calculations for turbulent vortex decay, have established these results as the expected long time behavior. Nonequilibrium flow with temporally decreasing turbulence intensity (eddy viscosity) yields other self similar solutions which decay slower than $t^{-1/2}$. When ν_T increases with time, as was the case in the present experiments, the vortex decay proceeds at a rate faster than $t^{-1/2}$. The low turbulence levels created by the airfoil in our tests resulted in conditions so far removed from equilibrium flow that the eddy viscosity increased steadily with time, thereby causing an accelerated rate of vortex decay. According to the data, the vortex could be considered decayed before it reached the slower equilibrium decay rate.

References

[1]Chigier, N.A. and Corsiglia, V.R., "Tip Vortices--Velocity Distributions," TM X-62,087, Sept. 1971, NASA.

[2]Chigier, N.A. and Corsiglia, V.R., "Wind Tunnel Studies of Wing Wake Turbulence," AIAA Paper 72-41, San Diego, Calif., Jan. 1972.

[3]Logan, A.H., "Vortex Velocity Distributions at Large Downstream Distance," Journal of Aircraft, Vol. 8, No. 11, Nov. 1971, pp. 930-932.

[4]Mason, W.H. and Marchman III, J.F., "Farfield Structure of an Aircraft Trailing Vortex, Including Effects of Mass Injection," CR-62078, April 1972, NASA.

[5]McCormick, B.W., Tangler, J.L., and Sherrieb, H.E., "Structure of Trailing Vortices," Journal of Aircraft, Vol. 5, No. 3, May-June 1968, pp. 260-267.

[6]Schraub, F.A., et al., "Use of Hydrogen Bubbles for Quantitative Determination of Time Dependent Velocity Fields in Low Speed Water Flows," Trans. Soc. Mech. Eng., Journal of Basic Engineering, Paper No. 64 - WA/FE-20, 1965.

[7]Orloff, K.L. and Grant, G.R., "The Application of a Laser Doppler Velocimeter to Trailing Vortex Definition and Alleviation," Paper presented at AIAA 6th Fluid and Plasma Dynamics Conference, Palm Springs, Calif., July 1973.

[8]Brown, C. E., "On the Aerodynamics of Wake Vortices," AIAA Journal, Vol. 11, No. 4, April 1973, pp. 531-536.

[9]Baldwin, B.S., Sheaffer, Y.S., and Chigier, N.A., "Prediction of Far Flow Field in Trailing Vortices,"AIAA Paper 72-989, Palo Alto, Calif., Sept. 1972.

[10]Govindraju, S.P. and Saffman, P.G., "Flow in a Turbulent Trailing Vortex," The Physics of Fluids, Vol. 14, No. 10, October, 1971, pp. 2074-2080.

[11]Hoffman, E.R. and Joubert, P.N., "Turbulent Line Vortices," Journal of Fluid Mechanics, Vol. 16, No. 3, July 1963, pp. 395-411.

[12]Donaldson, C. duP., "Calculation of Turbulent Shear Flows for Atmospheric and Vortex Motions," AIAA Journal, Vol. 10, No. 1, January 1972, pp. 4-12.

[13]Lamb, H., Hydrodynamics, 6th ed., Dover, New York, 1945, pp. 591-592.

[14]Corsiglia, V.R., Schwind, R., and Chigier, N.A., "Rapid Scanning, Three-Dimensional, Hot-Wire Anemometer Surveys for Wing-Tip Vortices in 40- by 80-Foot Wind Tunnel," AIAA Paper to be presented at

[15]Batchelor, G.K., "Axial Flow in Trailing Line Vortices," Journal of Fluid Mechanics, Vol. 20, Part 4, December 1964, pp. 645-658.

[16]Saffman, P.G., "Axial Flow in Laminar Trailing Vortex," Fluid Mechanics Seminar, Nov. 1972, Stanford Univ., Stanford, Calif.

[17]Owen, P.R., "The Decay of a Turbulent Trailing Vortex," The Aeronautical Quarterly, Vol. 21, Feb. 1970, pp. 69-78.

[18]Kuhn, G.D., and Nielsen, J.N., "Analytical Studies of Aircraft Trailing Vortices," AIAA Paper 72-42, San Diego, Calif., January 1972.

[19]Squire, H.B., "The Growth of a Vortex in Turbulent Flow," The Aeronautical Quarterly, Vol. 16, August 1965, pp. 302-306.

[20]Lilley, G.M., "A Note on the Decay of Aircraft Trailing Vortices," College of Aeronautics, Cranfield, England, Memo 22, 1964.

[21]Rose, R. and Dee, F.W., "Aircraft Vortex Wakes and Their Effects on Aircraft," Technical Note Aero 2934, December 1963, Royal Aircraft Establishment.

[22]Dosanjh, D.S., Gasparek, E.P., and Eskinazi, S., "Decay of a Viscous Trailing Vortex," The Aeronautical Quarterly, Vol. 13, May 1962, pp. 167-188.

[23]Newman, B.G., "Flow in a Viscous Trailing Vortex," The Aeronautical Quarterly, Vol. 10, May 1959, pp. 149-162.

[24]Templin, R.J., "Flow Characteristics in a Plane Behind the Trailing Edge of a Low Aspect Ratio Wing as Measured by a Special Pressure Probe," LM AE-58, 1954, NAE, Canada, (Quoted by Newman, B.G., in Ref. 23).

[25]Mabey, D.G., "The Formation and Decay of Vortices," DIC Thesis, 1953, Imperial College, London.

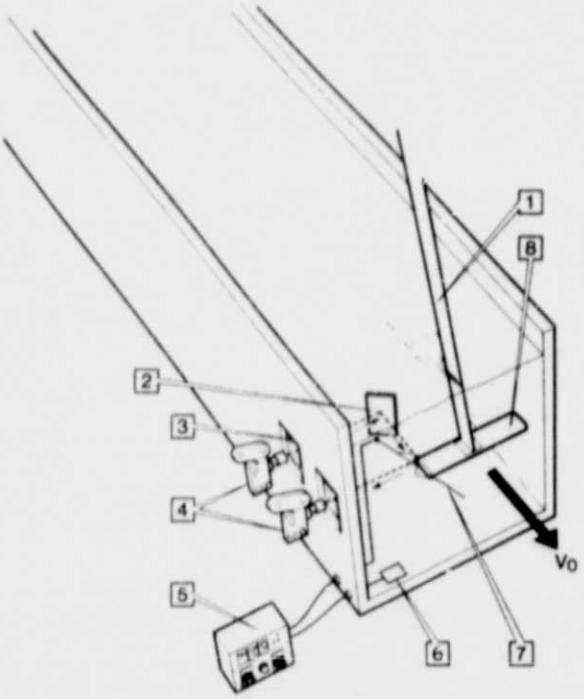

Fig. 1 Experimental set-up in towing tank: 1-strut, 2-mirror, 3-window, 4-cameras, 5-pulse generator, 6-ground plate, 7-H_2 bubbles, 8-airfoil.

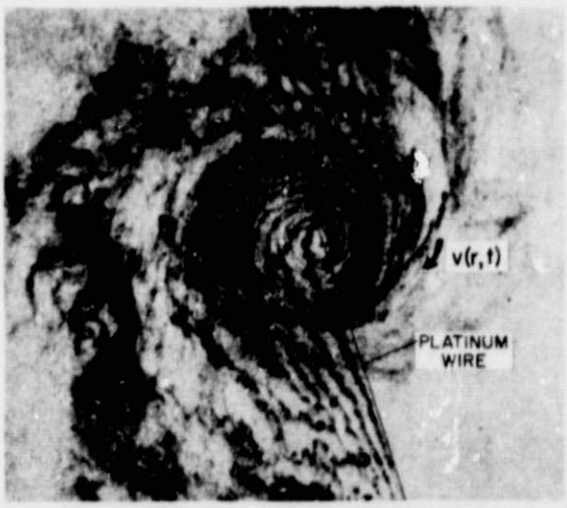

Fig. 2 Axial view of vortex field.

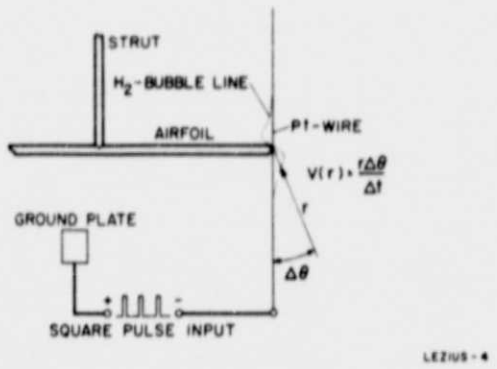

Fig. 3 Schematic of hydrogen bubble technique indicating determination of tangential velocity.

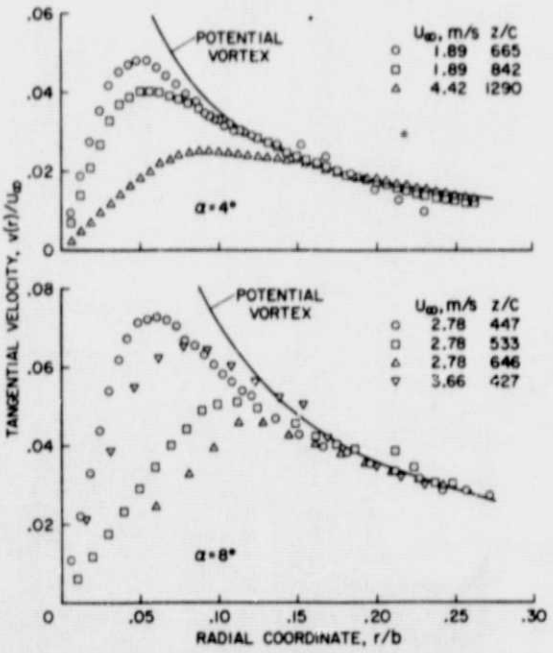

Fig. 4 Typical tangential velocity distributions as a function of downstream distance at 4° and 8° angles of attack.

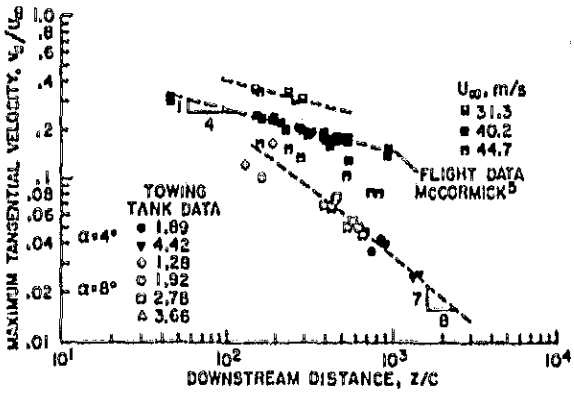

Fig. 5 Decay of maximum tangential velocity.

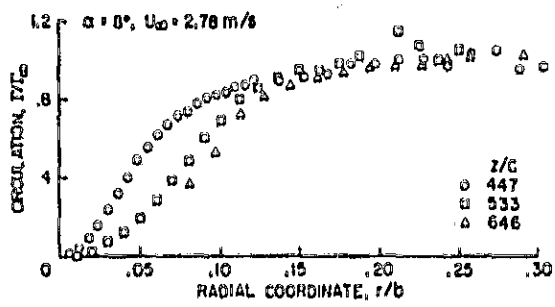

Fig. 7 Decay of circulation profiles with downstream distance.

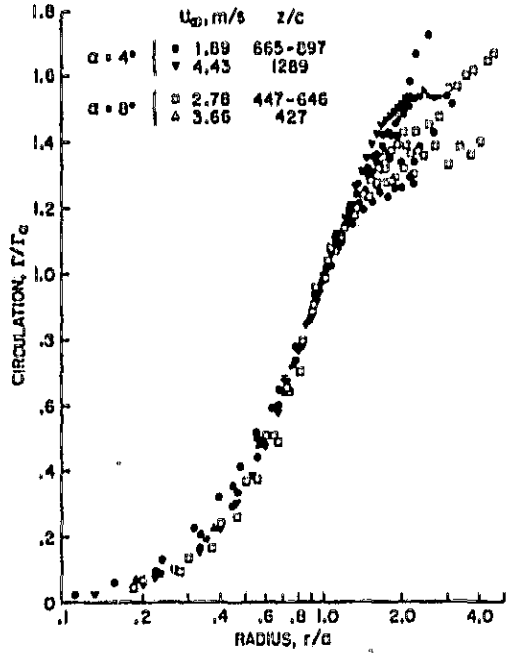

Fig. 8 Similarity plot of circulation profiles.

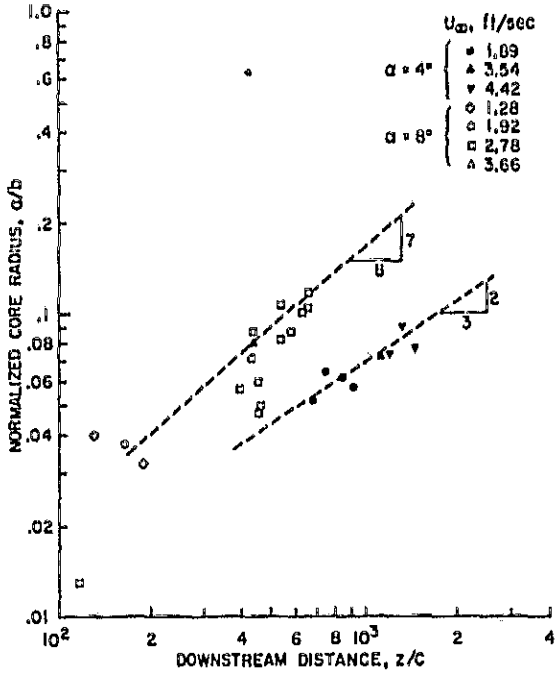

Fig. 6 Growth of core radius behind airfoil.

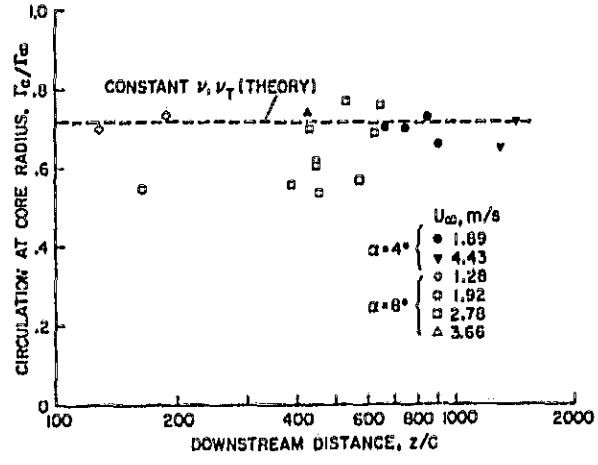

Fig. 9 Values of circulation determined at the core radius.

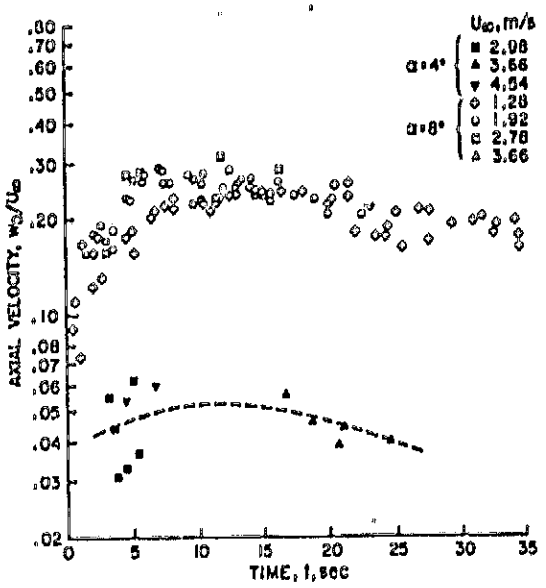

Fig. 10 Maximum axial velocity in towing direction after roll up.

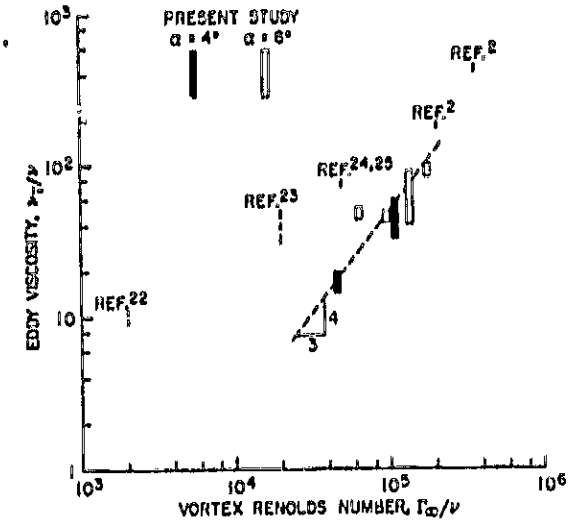

Fig. 12 Comparison of experimental eddy viscosity data.

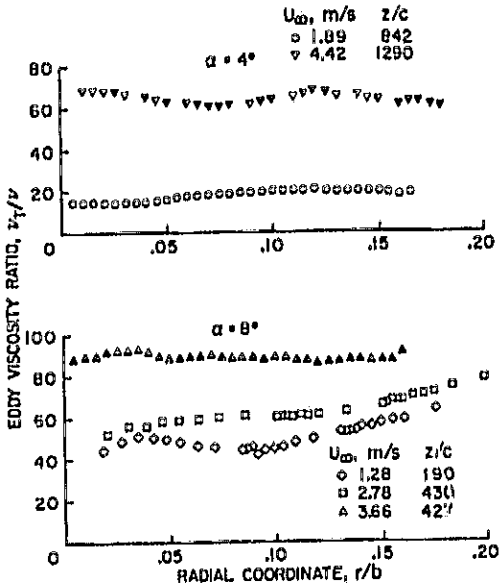

Fig. 11 Eddy viscosity profiles computed from experimental data and Eq. (17).

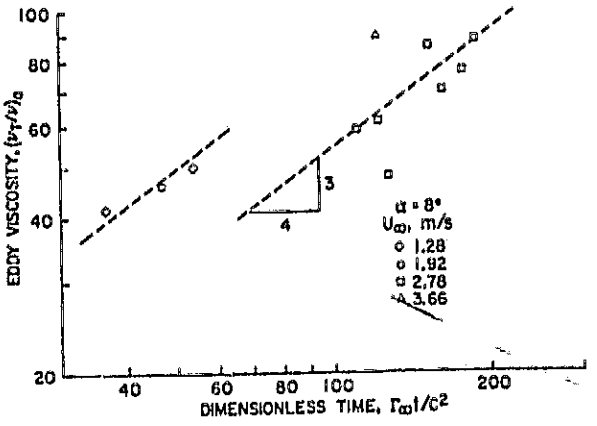

Fig. 13 Time dependence of eddy viscosity determined from data.

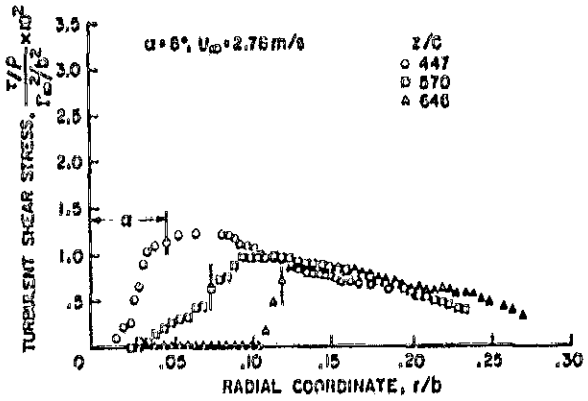

Fig. 14 Decay of turbulent shear stress profiles.

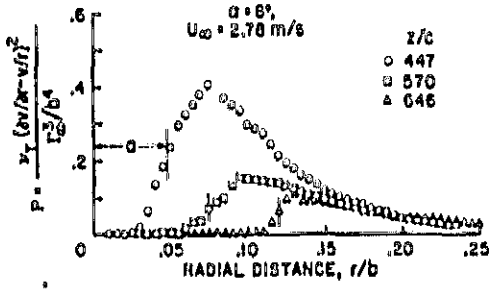

Fig. 15 Profiles of turbulent energy production.